The solution of the quenching puzzle within the microscopic approach to nuclear structure

Luigi Coraggio

Dipartimento di Matematica e Fisica - Università della Campania “Luigi Vanvitelli”
Istituto Nazionale di Fisica Nucleare - Sezione di Napoli

Multi-Aspect Young ORiented
Advanced Neutrino Academy 2025

June 16th 2025, Palazzo Grimaldi, Modica (RG)

Università degli Studi della Campania *Luigi Vanvitelli* — *Dipartimento di Matematica e Fisica*

INFN Istituto Nazionale di Fisica Nucleare

Acknowledgements

- University of Campania and INFN Naples Unit
  - G. De Gregorio
  - A. Gargano
  - N. Itaco
  - S. Lyu
  - L. C.
- INFN Pisa Unit
  - M. Viviani
- IPHC Strasbourg
  - F. Nowacki
- Peking University
  - F. R. Xu
  - Z. H. Chen
- FRIB
  - Y. Z. Ma

The quenching of g_A

A major issue in the calculation of quantities related to spin-isospin-dependent transitions is the need to quench the axial coupling constant g_A by a factor q in order to reproduce the data.

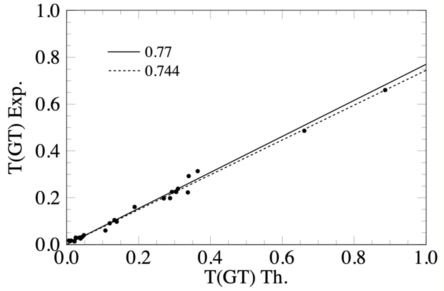

G. Martínez Pinedo et al., Phys. Rev. C **53**, *R2602 (1996)*

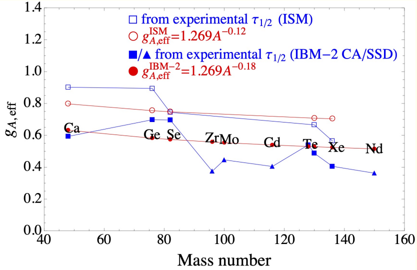

J. Barea, J. Kotila, and F. Iachello, Phys. Rev. C **91**, *034304 (2015)*

The quenching of g_A

This is an important question when studying $0\nu\beta\beta$ decay, in fact the need of a quenching factor q largely affects the value of the half-life $T^{0\nu}_{1/2}$, since the latter would be enlarged by a factor q^{-4}

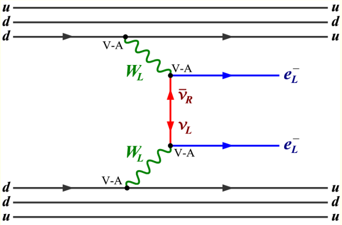

- The inverse of the $0\nu\beta\beta$-decay half-life is proportional to the squared nuclear matrix element $M^{0\nu}$

$$\left[T^{0\nu}_{1/2}\right]^{-1} = G^{0\nu}\left|M^{0\nu}\right|^2\left|g_A^2\frac{\langle m_\nu\rangle}{m_e}\right|^2$$

- $M^{0\nu}$ links $\left[T^{0\nu}_{1/2}\right]^{-1}$ to the neutrino effective mass $\langle m_\nu\rangle = \left|\sum_k m_k U^2_{ek}\right|$ (light-neutrino exchange)

That is why experimentalists are deeply concerned about q, its value has a strong impact on planning the sensitivity of the experimental apparatus.

The quenching of g_A

The two main sources of the need of a quenching factor q may be identified as:

Truncation of the nuclear configurations

Nuclear models operate a cut of the nuclear degrees of freedom in order to diagonalize the nuclear Hamiltonian $\Rightarrow$ effective Hamiltonians and decay operators must be considered to account for the neglected configurations in the nuclear wave function

Nucleon internal degrees of freedom

Nucleons are not point-like particles $\Rightarrow$ contributions to the free value of g_A come from two-body meson exchange currents:

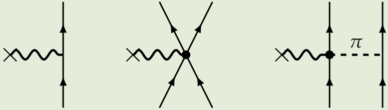

- *K. Shimizu, M. Ichimura, and A. Arima, Nucl. Phys. A* **226**, *282 (1974)*
- *I. S. Towner, Phys. Rep.* **155**, *263 (1987)*

The effective operators for decay amplitudes

- Ψ_α eigenstates of the full Hamiltonian H with eigenvalues E_α
- Φ_α eigenvectors obtained diagonalizing $H_{\rm eff}$ in the model space P and corresponding to the same eigenvalues E_α

$$\Rightarrow |\Phi_\alpha\rangle = P\,|\Psi_\alpha\rangle$$

Obviously, for any decay-operator Θ:

$$\langle \Phi_\alpha | \Theta | \Phi_\beta \rangle \neq \langle \Psi_\alpha | \Theta | \Psi_\beta \rangle$$

We then require an effective operator $\Theta_{\rm eff}$ defined as follows

$$\Theta_{\rm eff} = \sum_{\alpha\beta} |\Phi_\alpha\rangle \langle \Psi_\alpha | \Theta | \Psi_\beta \rangle \langle \Phi_\beta |$$

Consequently, the matrix elements of $\Theta_{\rm eff}$ are

$$\langle \Phi_\alpha | \Theta_{\rm eff} | \Phi_\beta \rangle = \langle \Psi_\alpha | \Theta | \Psi_\beta \rangle$$

This means that the parameters characterizing $\Theta_{\rm eff}$ are renormalized with respect to $\Theta \Rightarrow g_A^{\rm eff} = q \cdot g_A \neq g_A$

Two-body meson exchange currents

A powerful approach to the derivation of two-body currents (2BC) is to resort to effective field theories (EFT) of quantum chromodynamics.
In such a way, both nuclear potentials and 2BC may be consistently constructed, since in the EFT approach they appear as subleading corrections to the one-body Gamow-Teller (GT) operator $\sigma\tau^{\pm}$.

Nuclear Hamiltonian

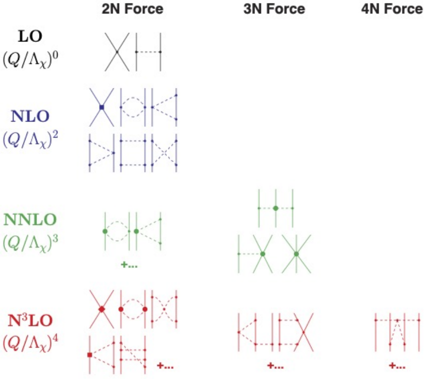

Two-body currents

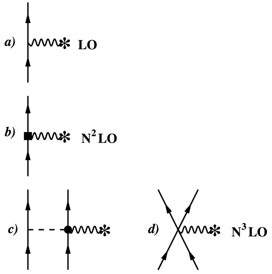

The impact of 2BC on the calculated β-decay properties has been investigated in terms of *ab initio* methods

β-decay in light nuclei

GT nuclear matrix elements of the β-decay of p-shell nuclei have been calculated with Green's function Monte Carlo (GFMC) and no-core shell model (NCSM) methods, including contributions from 2BC

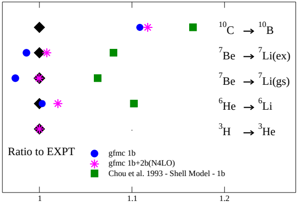

S. Pastore et al., Phys. Rev. C **97** 022501(R) (2018)

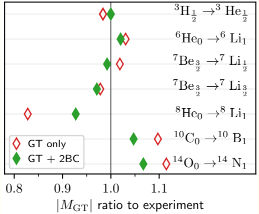

P. Gysbers et al., Nat. Phys. **15** 428 (2019)

The contribution of 2BC improves systematically the agreement between theory and experiment

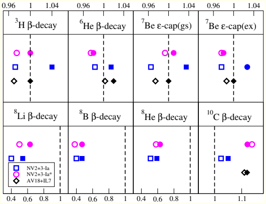

G. B. King et al., Phys. Rev. C **102** 025501 (2020)

Università degli Studi della Campania Luigi Vanvitelli — Dipartimento di Matematica e Fisica

INFN Istituto Nazionale di Fisica Nucleare

Ab initio methods: β-decay in medium-mass nuclei

Coupled-cluster method CCM and in-medium SRG (IMRSG) calculations have recently performed to overcome the quenching problem g_A to reproduce β-decay observables in heavier systems

P. Gysbers et al., Nat. Phys. **15** *428 (2019)*

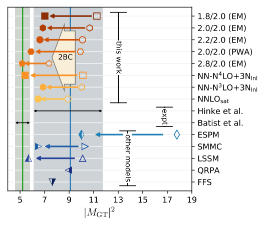

Coupled-Cluster Method

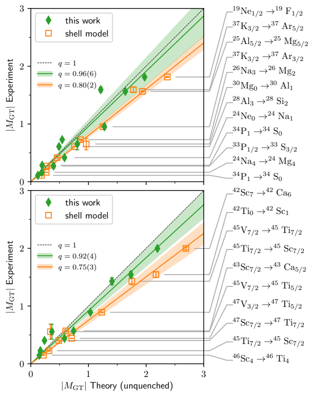

In-Medium SRG

A proper treatment of nuclear correlations and consistency between GT two-body currents and 3N forces, derived in terms of ChPT, explains the "quenching puzzle"

The realistic shell model

The nucleons are subject to the action of a mean field, that takes into account most of the interaction of the nuclear constituents.

Only valence nucleons interact by way of a residual two-body potential, within a reduced model space.

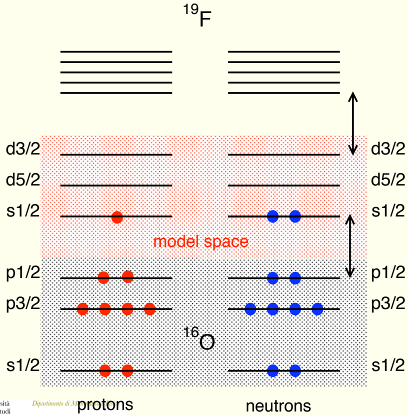

- Advantage → It is a microscopic and flexible model, the degrees of freedom of the valence nucleons are explicitly taken into account.
- Shortcoming → High-degree computational complexity.
- We perform our calculations employing the KSHELL shell-model code

Our approach to the realistic shell model

- Nuclear Hamiltonian: Entem-Machleidt N^{3}LO two-body potential plus N^{2}LO three-body potential

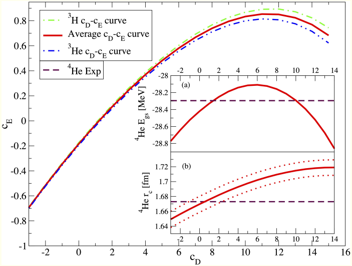

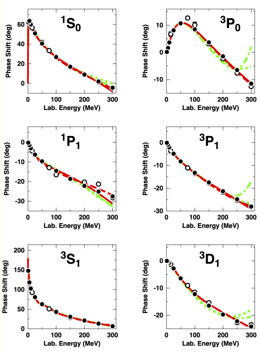

- Axial current $\mathbf{J}_A$ calculated at N^{3}LO in ChPT: LECs c_3, c_4, c_D are consistent with the 2NF and 3NF potentials
- $H_{\rm eff}$ calculated at 3rd order in perturbation theory
- Effective operators are consistently derived using MBPT

The effective shell-model Hamiltonian

We start from the many-body Hamiltonian H defined in the full Hilbert space:

$$H = H_0 + H_1 = \sum_{i=1}^{A} (T_i + U_i) + \sum_{i<j} (V_{ij}^{NN} - U_i)$$

$$\left(\begin{array}{c|c} PHP & PHQ \\ \hline QHP & QHQ \end{array} \right) \quad \begin{array}{c} \mathcal{H} = \Omega^{-1} H \Omega \\ \Longrightarrow \\ Q\mathcal{H}P = 0 \end{array} \quad \left(\begin{array}{c|c} P\mathcal{H}P & P\mathcal{H}Q \\ \hline 0 & Q\mathcal{H}Q \end{array} \right)$$

$$H_{\rm eff} = P\mathcal{H}P$$

Suzuki & Lee $\Rightarrow \Omega = e^{\omega}$ with $\omega = \left(\begin{array}{c|c} 0 & 0 \\ \hline Q\omega P & 0 \end{array} \right)$

$$H_1^{\rm eff}(\omega) = PH_1P + PH_1Q \frac{1}{\epsilon - QHQ} QH_1P -$$

$$- PH_1Q \frac{1}{\epsilon - QHQ} \omega H_1^{\rm eff}(\omega)$$

The perturbative approach to the shell-model H^{eff}

The $\hat{Q}$-box vertex function

$$\hat{Q}(\epsilon) = PH_1P + PH_1Q\frac{1}{\epsilon - QHQ}QH_1P$$

Exact calculation of the $\hat{Q}$-box is computationally prohibitive for many-body system $\Rightarrow$ we perform a perturbative expansion

$$\frac{1}{\epsilon - QHQ} = \sum_{n=0}^{\infty} \frac{(QH_1Q)^n}{(\epsilon - QH_0Q)^{n+1}}$$

$\hat{Q}$-box: 1st- & 2nd-order 1-b diagrams

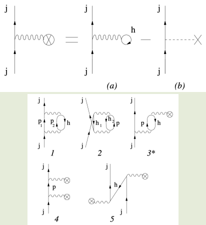

$\hat{Q}$-box: 1st- & 2nd-order 2-b diagrams

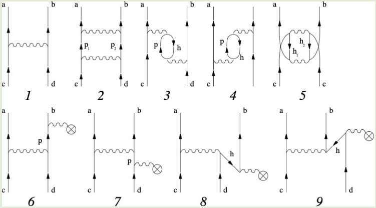

$0f1p$-shell nuclei

- Model space spanned by 4 proton and neutron orbitals $0f_{7/2}, 0f_{5/2}, 1p_{3/2}, 1p_{1/2}$
- Effects of induced 3-body forces have been included
- Single-particle energies and residual two-body interaction are derived from the theory. No empirical input

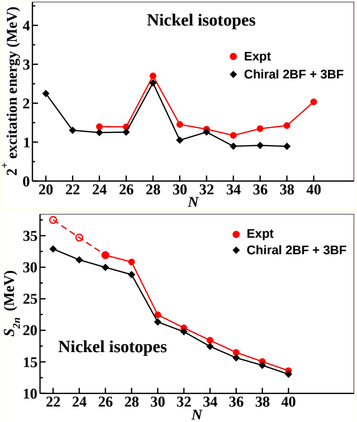

Y. Z. Ma, L. C., L. De Angelis, T. Fukui, A. Gargano, N. Itaco, and F. R. Xu, Phys. Rev. C **100***, 034324 (2019)*

$0f1p0g$-shell nuclei

- Model space spanned by 4 proton and neutron orbitals $0f_{5/2}, 1p_{3/2}, 1p_{1/2}, 0g_{9/2}$
- Effects of induced 3-body forces have been included
- Single-particle energies and residual two-body interaction are derived from the theory. No empirical input

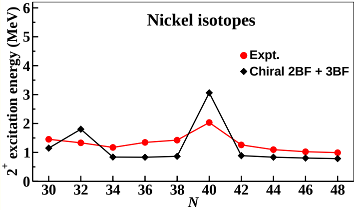

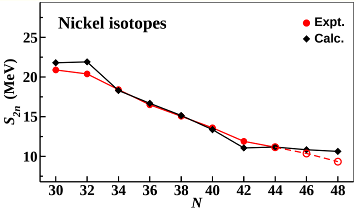

L. C., N. Itaco, G. De Gregorio, A. Gargano, Z. H. Cheng, Y. Z. Ma, F. R. Xu, and M. Viviani, Phys. Rev. C **109**, *014301 (2024)*

The effective SM operators for decay amplitudes

Any shell-model effective operator may be derived consistently with the $\hat{Q}$-box-plus-folded-diagram approach to $H_{\rm eff}$

It has been demonstrated that, for any bare operator Θ, a non-Hermitian effective operator $\Theta_{\rm eff}$ can be written in the following form:

$$\Theta_{\rm eff} = (P + \hat{Q}_1 + \hat{Q}_1 \hat{Q}_1 + \hat{Q}_2 \hat{Q} + \hat{Q} \hat{Q}_2 + \cdots)(\chi_0 + \\ + \chi_1 + \chi_2 + \cdots) \ ,$$

where

$$\hat{Q}_m = \frac{1}{m!} \frac{d^m \hat{Q}(\epsilon)}{d\epsilon^m} \bigg|_{\epsilon=\epsilon_0} \ ,$$

ϵ_0 being the model-space eigenvalue of the unperturbed Hamiltonian H_0

K. Suzuki and R. Okamoto, Prog. Theor. Phys. ***93*** *, 905 (1995)*

The effective SM operators for decay amplitudes

The χ_n operators are defined in terms of the vertex function $\hat{\Theta}$ as:

$$
\begin{aligned}
\chi_0 &= (\hat{\Theta}_0 + h.c.) + \Theta_{00} \quad , \\
\chi_1 &= (\hat{\Theta}_1 \hat{Q} + h.c.) + (\hat{\Theta}_{01} \hat{Q} + h.c.) \quad , \\
\chi_2 &= (\hat{\Theta}_1 \hat{Q}_1 \hat{Q} + h.c.) + (\hat{\Theta}_2 \hat{Q}\hat{Q} + h.c.) + \\
&\quad (\hat{\Theta}_{02} \hat{Q}\hat{Q} + h.c.) + \hat{Q}\hat{\Theta}_{11}\hat{Q} \quad , \\
&\quad \cdots
\end{aligned}
$$

and

$$
\hat{\Theta}(\epsilon) = P\Theta P + P\Theta Q \frac{1}{\epsilon - QHQ} QH_1 P
$$

$$
\hat{\Theta}(\epsilon_1;\epsilon_2) = PH_1 Q \frac{1}{\epsilon_1 - QHQ} \times Q\Theta Q \frac{1}{\epsilon_2 - QHQ} QH_1 P
$$

$$
\hat{\Theta}_m = \frac{1}{m!} \frac{d^m \hat{\Theta}(\epsilon)}{d\epsilon^m}\bigg|_{\epsilon=\epsilon_0}
$$

$$
\hat{\Theta}_{nm} = \frac{1}{n!m!} \frac{d^n}{d\epsilon_1^n} \frac{d^m}{d\epsilon_2^m} \hat{\Theta}(\epsilon_1;\epsilon_2)\bigg|_{\epsilon_{1,2}=\epsilon_0}
$$

The effective SM operators for decay amplitudes

The $\hat{\Theta}$-box is then calculated perturbatively, here are diagrams up to 2nd order of the effective decay operator $\Theta_{\rm eff}$ expansion:

One-body operator

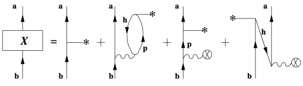

Two-body operator

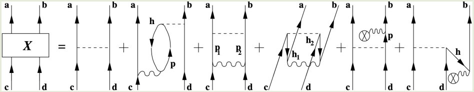

- *L. C., L. De Angelis, T. Fukui, A. Gargano, and N. Itaco, Phys. Rev. C* **95**,
- *L. C., L. De Angelis, T. Fukui, A. Gargano, N. Itaco, and F. Nowacki, Phys. Rev. C* **100**, *014316 (2019).*
- *L. C., A. Gargano, N. Itaco, R. Mancino, and F. Nowacki, Phys. Rev. C* **101**, *044315 (2020).*
- *L. C., N. Itaco, G. De Gregorio, A. Gargano, R. Mancino, and F. Nowacki, Phys. Rev. C* **105**, *034312 (2022).*

The axial current $\mathbf{J}_A$

The matrix elements of the axial current $\mathbf{J}_A$ are derived through a chiral expansion up to N^{3}LO, and employing the same LECs as in 2NF and 3NF

$$\mathbf{J}^{\rm LO}_{A,\pm} = -g_A \sum_i \boldsymbol{\sigma}_i \tau_{i,\pm} \ ,$$

$$\mathbf{J}^{\rm N^2LO}_{A,\pm} = \frac{g_A}{2m_N^2} \sum_i \mathbf{K}_i \times (\boldsymbol{\sigma}_i \times \mathbf{K}_i)\, \tau_{i,\pm} \ ,$$

$$\mathbf{J}^{\rm N^3LO}_{A,\pm}({\rm 1PE};\mathbf{k}) = \sum_{i<j} \frac{g_A}{2f_\pi^2} \Big\{ 4c_3 \tau_{j,\pm} \mathbf{k} + (\boldsymbol{\tau}_i \times \boldsymbol{\tau}_j)_\pm$$

$$\times \left[\left(c_4 + \frac{1}{4m} \boldsymbol{\sigma}_i \times \mathbf{k} - \frac{i}{2m} \mathbf{K}_i \right) \right] \Big\} \boldsymbol{\sigma}_j \cdot \mathbf{k} \frac{1}{\omega_k^2} \ ,$$

$$\mathbf{J}^{\rm N^3LO}_{A,\pm}({\rm CT};\mathbf{k}) = \sum_{i<j} z_0 (\boldsymbol{\tau}_i \times \boldsymbol{\tau}_j)_\pm (\boldsymbol{\sigma}_i \times \boldsymbol{\sigma}_j) \ ,$$

where

$$z_0 = \frac{g_A}{2f_\pi^2 m_N} \left[\frac{m_N}{4 g_a \Lambda_\chi} c_D + \frac{m_N}{3} (c_3 + 2c_4) + \frac{1}{6} \right] \ .$$

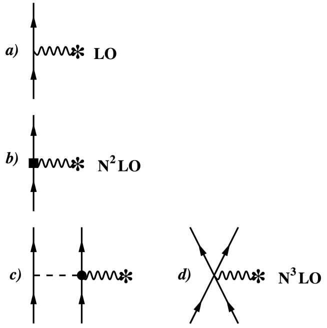

A. Baroni, L. Girlanda, S. Pastore, R. Schiavilla, and M. Viviani, Phys. Rev. C **93**, 015501 (2016)

Shell-model calculations and results

Nuclear model ⇒ Accurate reproduction of experimental data

⇓

Predictive power

RSM calculations, starting from ChPT two- and three-body potentials and two-body meson-exchange currents for spectroscopic and spin-isospin dependent observables of ^{48}Ca, ^{76}Ge, ^{82}Se

$\Downarrow$

Check RSM approach calculating GT strengths and $2\nu\beta\beta$-decay

$$\left[T^{2\nu}_{1/2}\right]^{-1} = G^{2\nu} \left|M^{2\nu}_{\rm GT}\right|^2$$

where

$$M^{\rm GT}_{2\nu} = \sum_n \frac{\langle 0^+_f || \mathbf{J}_A || 1^+_n \rangle \langle 1^+_n || \mathbf{J}_A || 0^+_i \rangle}{E_n + E_0}$$

$0f1p$-shell nuclei spectroscopic properties

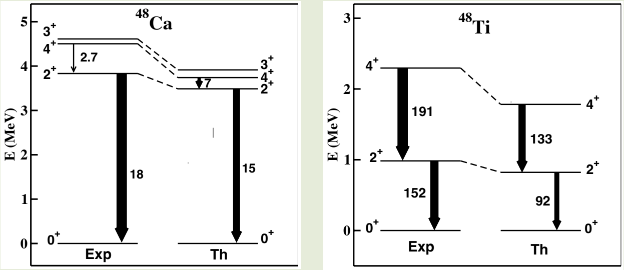

Nucleus	$J_i \rightarrow J_f$	bare	effective	$B(M1)_{\mathrm{Expt}}$
^{48}Ca				
	$3_1^+ \rightarrow 2_1^+$	0.090	0.044	0.023 ± 0.004

Nucleus	J^π	bare	effective	μ_{Expt}
^{48}Ti				
	2_1^+	0.26	0.34	$+0.78 \pm 0.04$
	4_1^+	1.0	1.1	$+2.2 \pm 0.5$

Gamow-Teller observables

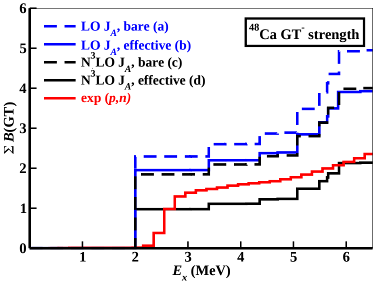

$$B(p,n) = \frac{|\langle \Phi_f || \sum \mathbf{J}_A || \Phi_i \rangle|^2}{2J_i + 1}$$

(a) bare $\mathbf{J}_A$ at LO in ChPT (namely the GT operator $g_A \boldsymbol{\sigma} \cdot \boldsymbol{\tau}$);

(b) effective $\mathbf{J}_A$ at LO in ChPT;

(c) bare $\mathbf{J}_A$ at N^3LO in ChPT (namely includy 2BC contributions too);

(d) effective $\mathbf{J}_A$ at N^3LO in ChPT.

Total GT$^-$ strength

	(a)	(b)	(c)	(d)	Expt
$\sum B(GT^-)$	24.0	17.5	20.9	11.2	15.3 ± 2.2

The impact of meson-exchange currents on the GT$^-$ matrix elements is $\approx 20\%$

Università degli Studi della Campania Luigi Vanvitelli — Dipartimento di Matematica e Fisica

INFN Istituto Nazionale di Fisica Nucleare

Gamow-Teller observables

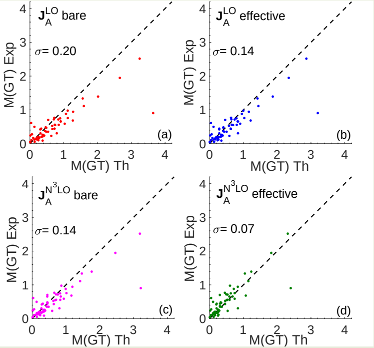

GT matrix elements of 60 experimental decays of 43 $0f1p$-shell nuclei, only yrast states involved

$$\sigma = \sqrt{\frac{\sum_{i=1}^{n}(x_i - \hat{x}_i)^2}{n}}$$

(a) bare $\mathbf{J}_A$ at LO in ChPT (namely the GT operator $g_A \boldsymbol{\sigma} \cdot \boldsymbol{\tau}$);

(b) effective $\mathbf{J}_A$ at LO in ChPT;

(c) bare $\mathbf{J}_A$ at N^3LO in ChPT (namely includy 2BC contributions too);

(d) effective $\mathbf{J}_A$ at N^3LO in ChPT.

$2\nu\beta\beta$ nuclear matrix element $M^{2\nu}$ $^{48}Ca \rightarrow ^{48}Ti$

$J_i^\pi \rightarrow J_f^\pi$	(a)	(b)	(c)	(d)	Expt
$0_1^+ \rightarrow 0_1^+$	0.057	0.048	0.033	0.019	0.042 ± 0.004
$0_1^+ \rightarrow 2_1^+$	0.131	0.102	0.097	0.057	≤ 0.023
$0_1^+ \rightarrow 0_2^+$	0.102	0.086	0.073	0.040	≤ 2.72

Università degli Studi della Campania Luigi Vanvitelli — Dipartimento di Matematica e Fisica

INFN Istituto Nazionale di Fisica Nucleare

$0f_{5/2}1p0g_{9/2}$-shell nuclei spectroscopic properties

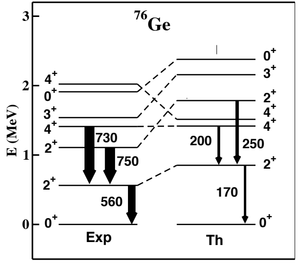

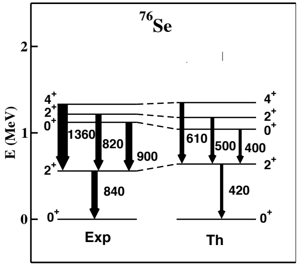

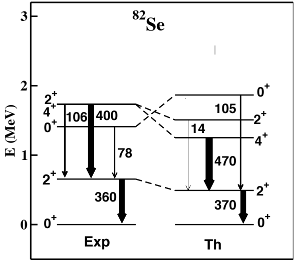

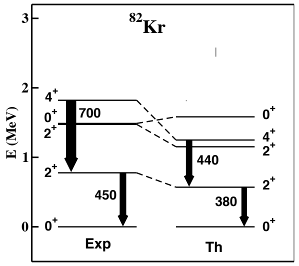

Università degli Studi della Campania Luigi Vanvitelli

Dipartimento di M

INFN Istituto Nazionale di Fisica Nucleare

Gamow-Teller observables

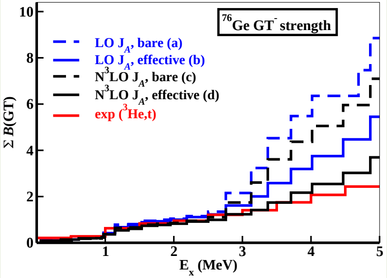

$$B(p,n) = \frac{|\langle \Phi_f || \sum \mathbf{J}_A || \Phi_i \rangle|^2}{2J_i + 1}$$

(a) bare $\mathbf{J}_A$ at LO in ChPT (namely the GT operator $g_A \boldsymbol{\sigma} \cdot \boldsymbol{\tau}$);

(b) effective $\mathbf{J}_A$ at LO in ChPT;

(c) bare $\mathbf{J}_A$ at N^{3}LO in ChPT (namely includy 2BC contributions too);

(d) effective $\mathbf{J}_A$ at N^{3}LO in ChPT.

Total GT$^-$ strength

	(a)	(b)	(c)	(d)	Expt
$\sum B(GT^-)$	15.8	10.8	12.8	7.4	$\sim$

The impact of meson-exchange currents on the GT$^-$ matrix elements is $\approx 18\%$

Gamow-Teller observables

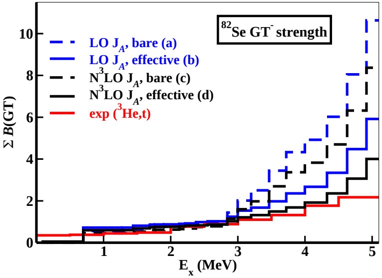

$$B(p,n) = \frac{|\langle \Phi_f || \sum \mathbf{J}_A || \Phi_i \rangle|^2}{2J_i + 1}$$

(a) bare $\mathbf{J}_A$ at LO in ChPT (namely the GT operator $g_A \boldsymbol{\sigma} \cdot \boldsymbol{\tau}$);

(b) effective $\mathbf{J}_A$ at LO in ChPT;

(c) bare $\mathbf{J}_A$ at N^{3}LO in ChPT (namely includy 2BC contributions too);

(d) effective $\mathbf{J}_A$ at N^{3}LO in ChPT.

Total GT$^-$ strength

	(a)	(b)	(c)	(d)	Expt
$\sum B(GT^-)$	19.0	11.4	14.9	7.5	$\sim$

The impact of meson-exchange currents on the GT$^-$ matrix elements is $\approx 20\%$

Gamow-Teller observables

$2\nu\beta\beta$ nuclear matrix element $M^{2\nu}$ ^{76}Ge$\rightarrow^{76}$Se

$J_i^\pi \rightarrow J_f^\pi$	(a)	(b)	(c)	(d)	Expt
$0_1^+ \rightarrow 0_1^+$	0.211	0.153	0.160	0.118	0.129 ± 0.004
$0_1^+ \rightarrow 2_1^+$	0.023	0.042	0.025	0.048	≤ 0.035
$0_1^+ \rightarrow 0_2^+$	0.009	0.086	0.016	0.063	≤ 0.089

$2\nu\beta\beta$ nuclear matrix element $M^{2\nu}$ ^{82}Se$\rightarrow^{82}$Kr

$J_i^\pi \rightarrow J_f^\pi$	(a)	(b)	(c)	(d)	Expt
$0_1^+ \rightarrow 0_1^+$	0.173	0.123	0.136	0.095	0.103 ± 0.001
$0_1^+ \rightarrow 2_1^+$	0.003	0.006	0.008	0.033	≤ 0.020
$0_1^+ \rightarrow 0_2^+$	0.018	0.007	0.013	0.007	≤ 0.052

L. C., N. Itaco, G. De Gregorio, A. Gargano, Z. H. Cheng, Y. Z. Ma, F. R. Xu, and M. Viviani, Phys. Rev. C **109**, *014301 (2024)*

Testing RSM: forbidden β-decay energy spectra

Forbidden β-decay logfts

Nucleus	bare	effective	Exp
^{94}Nb	11.30	11.58	11.95 (7)
^{99}Tc	11.580	11.876	12.325 (12)
^{113}Cd	21.902	22.493	23.127 (14)
^{115}In	21.22	21.64	22.53 (3)

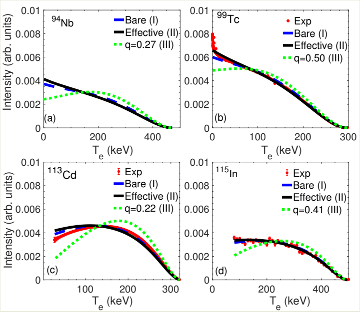

G. De Gregorio, R. Mancino, LC, N. Itaco, Phys. Rev. C **110**, *014324 (2024)*

Testing RSM: muon capture in *sd* shell nuclei

Spectroscopy of oxygen isotopes

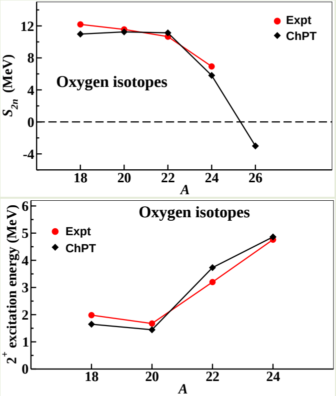

Running sums

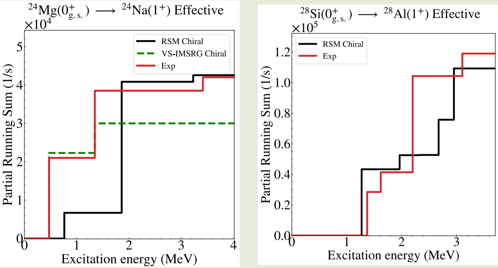

S. Lyu, G. De Gregorio, N. Itaco, LC, in preparation (2025)

Università degli Studi della Campania Luigi Vanvitelli — Dipartimento di Matematica e Fisica

INFN Istituto Nazionale di Fisica Nucleare

Conclusions and Outlook

- The role of many-body correlations prevails on the meson-exchange currents for the renormalization of GT operator, the latter contribute $\approx 20\%$
- The explanation of the "quenching puzzle" can be achieved by focusing theoretical efforts on two main goals:
  a) improving our knowledge of nuclear forces and exchange currents;
  b) deriving effective Hamiltonians and decay operators from many-body theory.
- We plan to expand soon our study by:
  - including meson-exchange two-body currents for the $M1$ transitions;
  - performing calculations for heavier-mass systems (^{100}Mo, ^{130}Te, ^{136}Xe);
  - calculating $0\nu\beta\beta$ decay $M^{0\nu}$ including also the LO contact term and three-nucleon exchange currents.

Università degli Studi della Campania Luigi Vanvitelli — Dipartimento di Matematica e Fisica

INFN Istituto Nazionale di Fisica Nucleare

Backup slides

Perturbative properties

Order-by-order convergence

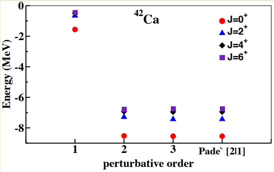

Intermediate-state convergence

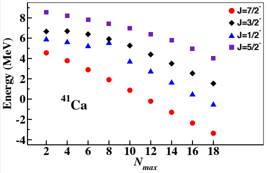

Intermediate-state convergence

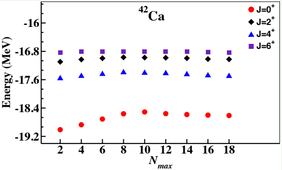

Y. Z. Ma, L. C., L. De Angelis, T. Fukui, A. Gargano, N. Itaco, and F. R. Xu, Phys. Rev. C **100**, *034324 (2019)*

Order-by-order convergence for $M^{2\nu}$ calculation

Decay	1st order	2nd order	3rd order	Expt.
^{130}Te $\rightarrow$ ^{130}Xe	0.142	0.040	0.044	0.034 ± 0.003
^{136}Xe $\rightarrow$ ^{136}Ba	0.0975	0.0272	0.0285	0.0218 ± 0.0003

Università degli Studi della Campania *Luigi Vanvitelli*

INFN Istituto Nazionale di Fisica Nucleare

Shell-evolution properties

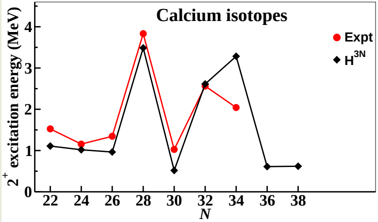

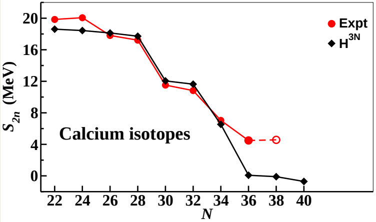

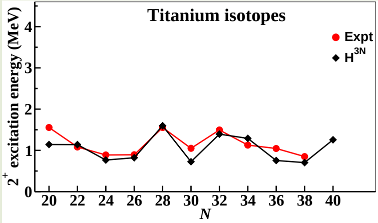

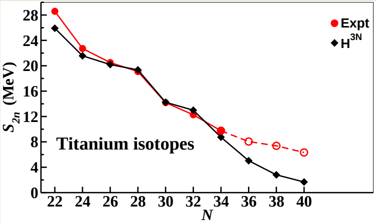

Induced three-body forces

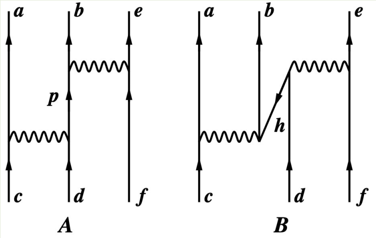

For many-valence nucleon systems (≥ 3) H_{eff} has to include the induced many-body components

Namely, at least three-body diagrams needs to be included in the perturbative expansion of the vertex function $\hat{Q}$ box

Shell model codes, at present, cannot manage three-body components of the shell-model Hamiltonian in large model spaces

We then resort to normal-ordering approximation, this means that TBME are different for each nuclear system

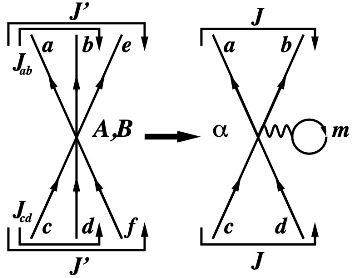

Results with CD-Bonn $V_{\text{low-}k}$

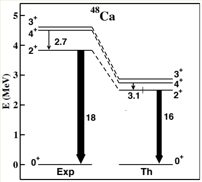

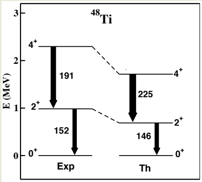

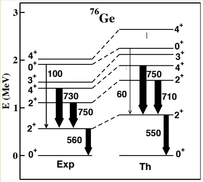

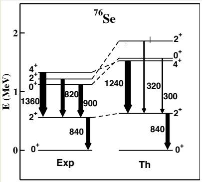

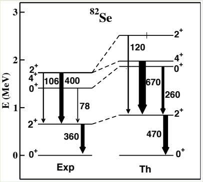

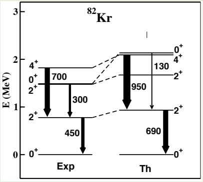

- *LC, L. De Angelis, T. Fukui, A. Gargano, N. Itaco, and F. Nowacki, Phys. Rev. C* **100***, 014316 (2019).*

Results with CD-Bonn $V_{\text{low-}k}$

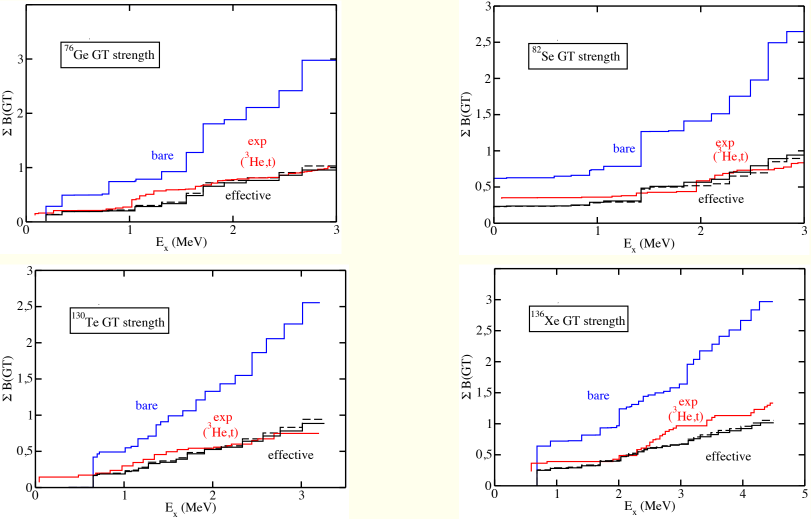

$$B(p,n) = \frac{\left|\langle \Phi_f || \sum_j \vec{\sigma}_j \tau_j^- || \Phi_i \rangle\right|^2}{2J_i + 1} \ , \quad (1)$$

Results with CD-Bonn $V_{\mathrm{low}\text{-}k}$

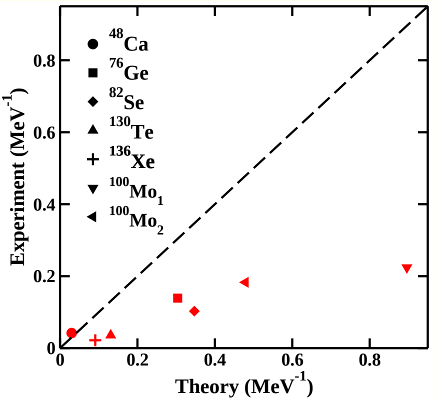

Red symbols: bare GT operator

Decay	Expt.	Bare
$^{48}\mathrm{Ca}_1 \rightarrow {}^{48}\mathrm{Ti}_1$	0.042 ± 0.004	0.030
$^{76}\mathrm{Ge}_1 \rightarrow {}^{76}\mathrm{Se}_1$	0.129 ± 0.005	0.304
$^{82}\mathrm{Se}_1 \rightarrow {}^{82}\mathrm{Kr}_1$	0.103 ± 0.001	0.347
$^{100}\mathrm{Mo}_1 \rightarrow {}^{100}\mathrm{Ru}_1$	0.224 ± 0.002	0.896
$^{100}\mathrm{Mo}_1 \rightarrow {}^{100}\mathrm{Ru}_2$	0.183 ± 0.006	0.479
$^{130}\mathrm{Te}_1 \rightarrow {}^{130}\mathrm{Xe}_1$	0.036 ± 0.001	0.131
$^{136}\mathrm{Xe}_1 \rightarrow {}^{136}\mathrm{Ba}_1$	0.0219 ± 0.0007	0.0910

Experimental data from *Thies et al, Phys. Rev. C* **86**, *044309 (2012); A. S. Barabash, Universe* **6**, *(2020)*

Results with CD-Bonn $V_{\text{low-}k}$

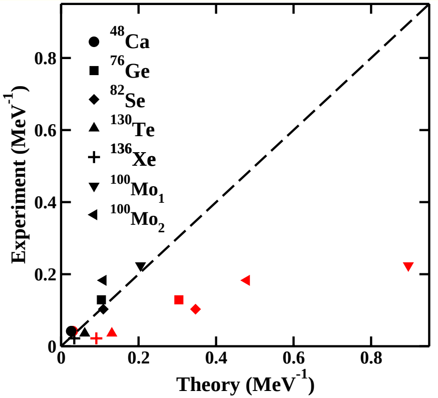

Red symbols: bare GT operator
Black symbols: effective GT operator

Decay	Expt.	Eff.
^{48}Ca$_1$ → ^{48}Ti$_1$	0.042 ± 0.004	0.026
^{76}Ge$_1$ → ^{76}Se$_1$	0.129 ± 0.005	0.104
^{82}Se$_1$ → ^{82}Kr$_1$	0.103 ± 0.001	0.109
^{100}Mo$_1$ → ^{100}Ru$_1$	0.224 ± 0.002	0.205
^{100}Mo$_1$ → ^{100}Ru$_2$	0.183 ± 0.006	0.109
^{130}Te$_1$ → ^{130}Xe$_1$	0.036 ± 0.001	0.061
^{136}Xe$_1$ → ^{136}Ba$_1$	0.0219 ± 0.0007	0.0341

Experimental data from *Thies et al, Phys. Rev. C* **86**, *044309 (2012); A. S. Barabash, Universe* **6**, *(2020)*

Decay	q
^{48}Ca → ^{48}Ti	0.83
^{76}Ge → ^{76}Se	0.58
^{82}Se → ^{82}Kr	0.56
^{100}Mo → ^{100}Ru	0.48
^{130}Te → ^{130}Xe	0.68
^{136}Xe → ^{136}Ba	0.61

- *LC, L. De Angelis, T. Fukui, A. Gargano, N. Itaco, and F. Nowacki, Phys. Rev. C* **100**, *014316 (2019).*
- *LC, N. Itaco, G. De Gregorio, A. Gargano, R. Mancino, and F. Nowacki, Phys. Rev. C* **105** *034312 (2022).*

Università degli Studi della Campania Luigi Vanvitelli
Dipartimento di Matematica e Fisica

INFN Istituto Nazionale di Fisica Nucleare